Linear dynamics of double-porosity dual-permeability materials. II. Fluid transport equations

Steven R. Pride*
Géosciences Rennes, Université de Rennes 1, 35042 Rennes Cedex, France

James G. Berryman†
University of California, Lawrence Livermore National Laboratory, P.O. Box 808 L-200, Livermore, California 94551-9900, USA

(Received 14 December 2002; published 9 September 2003)

For the purpose of understanding the acoustic attenuation of double-porosity composites, the key macroscopic equations are those controlling the fluid transport. Two types of fluid transport are present in double-porosity dual-permeability materials: (1) a scalar transport that occurs entirely within each averaging volume and that accounts for the rate at which fluid is exchanged between porous phase 1 and porous phase 2 when there is a difference in the average fluid pressure between the two phases and (2) a vector transport that accounts for fluid flux across an averaging region when there are macroscopic fluid-pressure gradients present. The scalar transport that occurs between the two phases can produce large amounts of wave-induced attenuation. The scalar transport equation is derived using volume-averaging arguments and the frequency dependence of the transport coefficient is obtained. The dual-permeability vector Darcy law that is obtained allows for fluid flux across each phase individually and is shown to have a symmetric permeability matrix. The nature of the cross coupling between the flow in each phase is also discussed.

DOI: 10.1103/PhysRevE.68.036604 PACS number(s): 43.20.+g, 81.05.Rm, 83.60.Uv, 83.60.Bc

I. INTRODUCTION

This is the second of two papers dedicated to obtaining macroscopic governing equations for double-porosity dual-permeability composite materials. In the first paper (Paper I), the governing equations were derived. The frequency dependence of the acoustic attenuation predicted from these equations depends strongly on the internal mesoscopic flow between the constituents. Thus, in this paper (Paper II), the fluid transport laws governing wave-induced fluid flow are studied in greater detail. The Biot theory of porous-media acoustics [1,2] ignores all wave-induced flow at mesoscopic scales. It is well known that Biot's theory is not capable of explaining the measured level of acoustic attenuation in porous rocks [3]. The theory developed in the present two papers provides one approach for doing so.

In Paper I [4], it was established in particular that the macroscopic governing equations controlling the linear response of isotropic double-porosity composites, when an $e^{-i\omega t}$ time dependence is assumed, take the form

$$\nabla\cdot\overline{\boldsymbol{\tau}}^{D}-\nabla\overline{p}_c=-i\omega(\rho\mathbf{v}+\rho_f\mathbf{q}_1+\rho_f\mathbf{q}_2)-\rho\mathbf{g}, \tag{1}$$

$$\begin{bmatrix}\mathbf{q}_1\\ \mathbf{q}_2\end{bmatrix}=-\frac{1}{\eta}\begin{bmatrix}\kappa_{11} & \kappa_{12}\\ \kappa_{12} & \kappa_{22}\end{bmatrix}\begin{bmatrix}\nabla\overline{p}_{f1}-\rho_f(i\omega\mathbf{v}+\mathbf{g})\\ \nabla\overline{p}_{f2}-\rho_f(i\omega\mathbf{v}+\mathbf{g})\end{bmatrix}, \tag{2}$$

$$\frac{1}{i\omega}\begin{bmatrix}\nabla\cdot\mathbf{v}\\ \nabla\cdot\mathbf{q}_1\\ \nabla\cdot\mathbf{q}_2\end{bmatrix}=\begin{bmatrix}a_{11} & a_{12} & a_{13}\\ a_{12} & a_{22} & a_{23}\\ a_{13} & a_{23} & a_{33}\end{bmatrix}\begin{bmatrix}\overline{p}_c\\ \overline{p}_{f1}\\ \overline{p}_{f2}\end{bmatrix}+\begin{bmatrix}0\\ \zeta_{\rm int}\\ -\zeta_{\rm int}\end{bmatrix}, \tag{3}$$

$$-i\omega\zeta_{\rm int}=\gamma(\omega)(\overline{p}_{f1}-\overline{p}_{f2}), \tag{4}$$

$$-i\omega\overline{\boldsymbol{\tau}}^{D}=[G-i\omega F]\left[\nabla\mathbf{v}+(\nabla\mathbf{v})^{T}-\frac{2}{3}\nabla\cdot\mathbf{v}\mathbf{I}\right]. \tag{5}$$

See Paper I for the definition of the various fields. What needs to be established further in the present paper is the detailed nature of transport coefficients in Eqs. (2) and (4).

As demonstrated in Paper I, only two aspects of the macroscopic fluid pressure response are driving fluid transport in this theory: (1) the difference between the average fluid pressures in each phase $\overline{p}_{f1}-\overline{p}_{f2}$ is responsible for the scalar transport $\dot{\zeta}_{\rm int}$ internal to Ω; and (2) the average drop in fluid pressure from one side of a constituent averaging region to the other $\nabla\overline{p}_{f1}$ and $\nabla\overline{p}_{f2}$ is responsible for the vector transport $\mathbf{q}_i$ across Ω_i. For the isotropic composites being treated here, there is no coupling between the tensorial orders of the flow [5]. Due to the linearity of the physics, we choose to resolve the fluid transport into a scalar part defined with $\overline{p}_{fi}\neq 0$ and $\nabla\overline{p}_{fi}=\mathbf{0}$, for $i=1,2$, that defines the internal transfer between the constituents, and into a vector part in which $\overline{p}_{fi}=0$ and $\nabla\overline{p}_{fi}\neq\mathbf{0}$ that defines the macroscopic (Darcy) flow within each constituent. The sum of these two contributions gives the total fluid transport within (and across) each averaging volume Ω.

Section II presents the analysis of the internal fluid transport in the composite double-porosity medium. Section III presents the macroscopic flow laws. Our conclusions are summarized in the final section. A technical appendix describes a specific model calculation used to motivate some of the conclusions in Sec. III.

II. INTERNAL FLUID TRANSFER

In what follows, the internal fluid transfer $\dot{\zeta}_{\rm int}$ is shown to obey a transport law of the form

*Email address: spride@univ-rennes1.fr
†Email address: berryman1@llnl.gov

$$\dot{\zeta}_{\rm int}=\int_0^\infty dt'\Gamma(t')[\overline{p}_{f1}(t-t')-\overline{p}_{f2}(t-t')], \tag{6}$$

as has already been anticipated from the statement of the energy-dissipation rate given in Eq. (42) of Paper I. The relaxation function $\Gamma(t)$ can be expressed as

$$\Gamma(t)=\frac{1}{2\pi}\int_{-\infty}^{\infty}d\omega\gamma(\omega)e^{-i\omega t}, \tag{7}$$

so that in the frequency domain this transport law takes the form [Eq. (71) of Paper I]

$$-i\omega\zeta_{\rm int}(\omega)=\gamma(\omega)[\overline{p}_{f1}(\omega)-\overline{p}_{f2}(\omega)], \tag{8}$$

i.e., such internal transport occurs to the extent that the average fluid pressures in each phase are different.

We determine the transport coefficient $\gamma(\omega)$ by treating the particular situation in which a sealed sample of the composite is immersed in a reservoir whose pressure may be controlled. Such an isolated sealed sample will have no net macroscopic fluid flux across either phase ($\mathbf{q}_i=\mathbf{0}$), which is equivalent to the desired macroscopic conditions of $\nabla\overline{p}_{fi}=\mathbf{0}$. The approach taken to determine $\gamma(\omega)$ is essentially that of Johnson *et al.* [6]. The idea is to determine the nature of $\dot{\zeta}_{\rm int}$ in the limit of both low and high frequencies and then to connect the frequency dependence in these two limits by a simple postulated function of frequency satisfying causality constraints. Johnson [7] has also recently applied very similar ideas to the problem of patchy saturation in porous media.

Assuming that a sealed sample Ω of the double-porosity composite is immersed in a fluid reservoir whose pressure varies in time as $\Delta Pe^{-i\omega t}$, the local fluid pressures p_{fi} in each phase $i=1,2$ are determined from the following diffusion problem [obtained from Eqs. (1)–(4) of Paper I with definitions of the various local fields as given there]:

$$\frac{k_i}{\eta}\nabla^2 p_{fi}+i\omega\frac{\alpha_i}{K_iB_i}p_{fi}=i\omega\frac{\alpha_i}{K_i}p_{ci}, \tag{9}$$

subject to the sealed-sample boundary condition

$$\mathbf{n}\cdot\nabla p_{fi}=0 \quad \text{on} \quad \partial\Omega_i, \tag{10}$$

and to the continuity conditions

$$[p_{fi}]=0$$

and

$$[k_i\mathbf{n}\cdot\nabla p_{fi}]=0 \quad \text{on} \quad \partial\Omega_{12}. \tag{11}$$

The square brackets in the continuity conditions mean to evaluate the jump in the stated quantity across the interface. As in Paper I, the sample volume is being partitioned into phase 1 and phase 2 portions $\Omega=\Omega_1+\Omega_2$ as is the external surface of the sample $\partial\Omega=\partial\Omega_1+\partial\Omega_2$. The internal surface separating the two phases are again denoted by $\partial\Omega_{12}$.

In general, when the two phases have arbitrary geometry and elastic properties, the local confining pressure changes p_{ci} acting as the source term in Eq. (9) need not be uniform throughout their respective regions. To determine the p_{ci}, the following equations are therefore required:

$$\nabla\cdot\boldsymbol{\tau}_i^D=\nabla p_{ci}, \tag{12}$$

$$\boldsymbol{\tau}_i^D=G_i[\nabla\mathbf{u}_i+\nabla\mathbf{u}_i^T-\tfrac{2}{3}\nabla\cdot\mathbf{u}_i\mathbf{I}], \tag{13}$$

$$p_{ci}=-K_i\nabla\cdot\mathbf{u}_i+\alpha_i p_{fi}, \tag{14}$$

subject to the boundary conditions

$$\mathbf{n}\cdot(\boldsymbol{\tau}_i^D-p_{ci}\mathbf{I})=-\mathbf{n}\Delta P \quad \text{on} \quad \partial\Omega_i, \tag{15}$$

$$[\mathbf{u}_i]=0$$

and

$$[\mathbf{n}\cdot(\boldsymbol{\tau}_i^D-p_{ci}\mathbf{I})]=0 \quad \text{on} \quad \partial\Omega_{12}. \tag{16}$$

This set of differential equations [Eqs. (9)–(16)] is what controls the local internal fluid transfer.

A. Low-frequency limit

In the limit as $\omega\to 0$, the above fields may be developed as perturbation expansions in $-i\omega$,

$$p_{fi}=p_{fi}^{(0)}-i\omega p_{fi}^{(1)}+O(\omega^2), \tag{17}$$

$$p_{ci}=p_{ci}^{(0)}-i\omega p_{ci}^{(1)}+O(\omega^2), \tag{18}$$

and equivalently for $\mathbf{u}_i$ and $\boldsymbol{\tau}_i^D$. Note, however, that the total confining pressure $\overline{p}_c=v_1\overline{p}_{c1}+v_2\overline{p}_{c2}=\Delta P$ is independent of frequency.

The zero-order fluid pressure response is governed by

$$\nabla^2 p_{fi}^{(0)}=0, \tag{19}$$

$$\mathbf{n}\cdot\nabla p_{fi}^{(0)}=0 \quad \text{on} \quad \partial\Omega_i, \tag{20}$$

$$[k_i\mathbf{n}\cdot\nabla p_{fi}^{(0)}]=0$$

and

$$[p_{fi}]=0 \quad \text{on} \quad \partial\Omega_{12}. \tag{21}$$

This boundary-value problem has the unique solution $p_{f1}^{(0)}=p_{f2}^{(0)}=B_o\Delta P$ (a uniform constant).

To determine B_o (the zero-frequency or "single porosity" Skempton's coefficient [8] of the composite), the second and third lines of Eq. (3) are added under sealed conditions ($\nabla\cdot\mathbf{q}_i=0$) to obtain

$$0=(a_{12}+a_{13})\overline{p}_c+(a_{22}+a_{23})\overline{p}_{f1}+(a_{23}+a_{33})\overline{p}_{f2}, \tag{22}$$

where a_{ij} are given by Eqs. (64)–(69) of Paper I. If the perturbation expansions for the fluid pressures are introduced and if terms are grouped by common factors of $-i\omega$, one obtains

$$\frac{\overline{p_{fi}^{(0)}}}{\Delta P} \equiv B_o = -\frac{a_{12}+a_{13}}{a_{22}+2a_{23}+a_{33}}, \tag{23}$$

$$\frac{\overline{p_{f2}^{(1)}}}{\overline{p_{f1}^{(1)}}} = -\frac{a_{22}+a_{23}}{a_{33}+a_{23}}. \tag{24}$$

However, Eq. (24) will not be needed in what follows.

The leading-order correction to uniform fluid pressure is thus governed by the Poisson problem

$$\frac{k_i}{\eta}\nabla^2 p_{fi}^{(1)} = \frac{\alpha_i}{K_i}\left[p_{ci}^{(0)} - \frac{B_o}{B_i}\Delta P\right], \tag{25}$$

subject to the previously stated no-flow condition on $\partial\Omega_i$ and continuity conditions on $\partial\Omega_{12}$. The zero-order confining pressure that acts as the source term is given by

$$p_{ci}^{(0)} = -K_i \nabla\cdot\mathbf{u}_i^{(0)} + \alpha_i B_o \Delta P. \tag{26}$$

The displacement fields $\mathbf{u}_i^{(0)}$ are now scaled as

$$\mathbf{u}_i^{(0)}(\mathbf{r}) = -\frac{1-\alpha_i B_o}{K_i}\Delta P \mathbf{s}_i(\mathbf{r}), \tag{27}$$

where $\mathbf{s}_i$ are applied-pressure-independent displacement fields satisfying the well-posed problem

$$\mu_i \nabla^2 \mathbf{s}_i + \left(1+\frac{\mu_i}{3}\right)\nabla\nabla\cdot\mathbf{s}_i = 0 \quad \text{in} \quad \Omega_i, \tag{28}$$

subject to the boundary conditions on $\partial\Omega_i$

$$\mu_i \mathbf{n}\cdot\left(\nabla\mathbf{s}_i + \nabla\mathbf{s}_i^T - \frac{2}{3}\nabla\cdot\mathbf{s}\mathbf{I}\right) + (1-\alpha_i B_o)\nabla\cdot\mathbf{s}_i\mathbf{n} = (1-\alpha_i B_o)\mathbf{n}, \tag{29}$$

and to the two continuity conditions across $\partial\Omega_{12}$

$$\left[\mu_i \mathbf{n}\cdot\left(\nabla\mathbf{s}_i + \nabla\mathbf{s}_i^T - \frac{2}{3}\nabla\cdot\mathbf{s}\mathbf{I}\right) + (1-\alpha_i B_o)\nabla\cdot\mathbf{s}_i\mathbf{n} + \alpha_i B_o \mathbf{n}\right] = 0, \tag{30}$$

$$\left[\frac{1-\alpha_i B_o}{K_i}\mathbf{s}_i\right] = \mathbf{0}. \tag{31}$$

A dimensionless shear modulus $\mu_i \equiv (1-\alpha_i B_o)G_i/K_i$ has been introduced. Such scaling of the displacements results in $|\nabla\cdot\mathbf{s}_i| \approx O(1)$, as is seen in Eqs. (28) and (29).

Having established these results, we can now address the low-frequency behavior of $\dot{\zeta}_{\text{int}}$. As $\omega\to 0$, the definition of $\dot{\zeta}_{\text{int}}$ [Eq. (27) of Paper I] along with the fact that $\nabla p_{fi}^{(0)} = \mathbf{0}$, so that to leading order in $-i\omega$ we have $\mathbf{n}\cdot\mathbf{q}_{12} = i\omega k_1 \mathbf{n}\cdot\nabla p_{f1}^{(1)}/\eta = i\omega k_2 \mathbf{n}\cdot\nabla p_{f2}^{(1)}/\eta$ on $\partial\Omega_{12}$, defines the integral

$$-i\omega\zeta_{\text{int}} = \frac{i\omega}{V}\frac{k_1}{\eta}\int_{\partial\Omega_{12}} \mathbf{n}\cdot\nabla p_{f1}^{(1)} dS + O(\omega^2). \tag{32}$$

This integral is obtained by integrating Eq. (25) over all of Ω_1 and applying the divergence theorem

$$\frac{k_1}{\eta}\frac{1}{V}\int_{\partial\Omega_{12}} \mathbf{n}\cdot\nabla p_{f1}^{(1)} dS = \frac{\alpha_1}{K_1} v_1 \left(\overline{p_{c1}^{(0)}} - \frac{B_o}{B_1}\Delta P\right). \tag{33}$$

If Eq. (55) of Paper I is used for $\overline{p_{c1}^{(0)}}$ along with the facts that $\overline{p_c} = \Delta P$ and $\overline{p_{f1}^{(0)}} = \overline{p_{f2}^{(0)}} = B_o \Delta P$, the exact low-frequency limit is obtained as

$$-i\omega\zeta_{\text{int}} = -i\omega[a_{12} + B_o(a_{22}+a_{23})]\Delta P + O(\omega^2). \tag{34}$$

It has been verified algebraically that this result is unchanged if throughout Eq. (33), the index 1 is replaced by 2 and $\mathbf{n}$ is replaced by $-\mathbf{n}$.

The next step needed in order to define the transport coefficient $\gamma(\omega)$ requires us to replace $-i\omega\Delta P$ by $\overline{p_{f1}} - \overline{p_{f2}}$. An average of Eq. (17) gives

$$\overline{p_{f1}} - \overline{p_{f2}} = -i\omega(\overline{p_{f1}^{(1)}} - \overline{p_{f2}^{(1)}}) + O(\omega^2). \tag{35}$$

Because Eqs. (25)–(31) governing the response $p_{fi}^{(1)}$ are linear in ΔP, we can define a ΔP independent material property Υ as

$$\Upsilon = \frac{\overline{p_{f1}^{(1)}} - \overline{p_{f2}^{(1)}}}{\Delta P}. \tag{36}$$

Thus, in the transport law $-i\omega\zeta_{\text{int}} = \gamma_o[\overline{p_{f1}} - \overline{p_{f2}}] + O(\omega^2)$, we can identify the low-frequency transport coefficient $\gamma_o = \lim_{\omega\to 0}\gamma(\omega)$ as

$$\gamma_o = [a_{12} + B_o(a_{22}+a_{23})]/\Upsilon. \tag{37}$$

However, for the theory to be useful, the material property dependencies of Υ need to be specified. To do so analytically requires approximations to be invoked.

In practice, phase 2 is envisioned to be either small pockets embedded within a larger body of phase 1 material or to be in the form of thin through-going joints. In the idealization that either the pockets can be modeled as ellipsoids or that the joints are planar (and have intersection volumes that can be considered negligible), Eqs. (28)–(31) are solved exactly by the deformation tensor $\nabla\mathbf{s}_i = \mathbf{I}/3$, with $\nabla\cdot\mathbf{s}_i = 1$, which corresponds to uniform confining pressure throughout both phases. Using this approximation, the equations governing $p_{fi}^{(1)}$ can be written as

$$\frac{k_1}{\eta}\nabla^2 p_{f1}^{(1)} = \left(1-\frac{B_o}{B_1}\right)\frac{\alpha_1}{K_1}\Delta P \quad \text{in} \quad \Omega_1, \tag{38}$$

$$\frac{k_1}{\eta}\nabla^2 p_{f2}^{(1)} = \frac{k_1}{k_2}\left(1-\frac{B_o}{B_2}\right)\frac{\alpha_2}{K_2}\Delta P \quad \text{in} \quad \Omega_2, \tag{39}$$

with the boundary conditions

$$\mathbf{n}\cdot\nabla p_{fi}^{(1)} = 0 \quad \text{on} \quad \partial\Omega_i, \tag{40}$$

$$\mathbf{n}\cdot\nabla p_{f2}^{(1)}=\frac{k_1}{k_2}\mathbf{n}\cdot\nabla p_{f1}^{(1)} \quad \text{on} \quad \partial\Omega_{12}, \tag{41}$$

$$p_{f1}^{(1)}=p_{f2}^{(1)} \quad \text{on} \quad \partial\Omega_{12}, \tag{42}$$

where the right-hand sides of Eqs. (38) and (39) are now spatially uniform constants.

To simplify further, we now use the fact that the permeability ratio k_1/k_2 can be considered a small number in almost any application where a dual-permeability model is likely to be necessary. In the $k_1/k_2\to 0$ limit, the phase 2 response $p_{f2}^{(1)}(\mathbf{r})=\overline{p_{f2}^{(1)}}$ becomes a spatial constant. The phase 1 response can then be written as

$$p_{f1}^{(1)}(\mathbf{r})=\overline{p_{f2}^{(1)}}-\frac{\eta}{k_1}\left(1-\frac{B_o}{B_1}\right)\frac{\alpha_1}{K_1}\Delta P\Phi_1(\mathbf{r}), \tag{43}$$

where the potential $\Phi_1(\mathbf{r})$ has units of length squared and satisfies the purely geometric problem

$$\nabla^2\Phi_1=-1 \quad \text{in} \quad \Omega_1, \tag{44}$$

$$\mathbf{n}\cdot\nabla\Phi_1=0 \quad \text{on} \quad \partial\Omega_1, \tag{45}$$

$$\Phi_1=0 \quad \text{on} \quad \partial\Omega_{12}. \tag{46}$$

In analogy to Johnson's treatment [7] of patchy saturation, since Φ_1 has units of length squared, a length L_1 is introduced by defining

$$L_1^2\equiv\frac{1}{V_1}\int_{\Omega_1}\Phi_1 dV=\frac{1}{V_1}\int_{\Omega_1}\nabla\Phi_1\cdot\nabla\Phi_1 dV. \tag{47}$$

Multiplying both sides of Eq. (44) with Φ_1 and then integrating easily demonstrates the equality of the integrals in Eq. (47). The length L_1 defines the average distance over which the fluid-pressure gradient still exists in phase 1 in the final stages of equilibration. With these results, Υ can be written as

$$\Upsilon=-\frac{\eta}{k_1}\left(1-\frac{B_o}{B_1}\right)\frac{\alpha_1}{K_1}L_1^2 \tag{48}$$

to leading order in k_1/k_2.

The same geometric approximation $\nabla\cdot\mathbf{s}_i=1$ that yielded Eq. (48) for Υ, also requires the composite's drained bulk modulus to be the harmonic mean $1/K=v_1/K_1+v_2/K_2$ in which case $Q_1=Q_2=1$. Because of this, the numerator in $\gamma_o=[a_{12}+B_o(a_{22}+a_{23})]/\Upsilon$ can be further reduced allowing γ_o to be expressed in the final form

$$\gamma_o=\frac{v_1 k_1}{\eta L_1^2}. \tag{49}$$

The dependence on the mesoscopic geometry of the two phases enters through L_1.

In the special case in which phase 2 is a small sphere of radius $r=a$ surrounded by a spherical shell of phase 1, so that the composite sphere has a total radius of $r=R$ (i.e., phase 1 lies within $a<r<R$), we can determine Φ_1 by integrating the Laplace equation Green function over phase 1. The Green function ψ satisfying $\nabla^2\psi=-\delta(\mathbf{r}-\mathbf{r}_o)$ and the boundary conditions of $\partial\psi/\partial r=0$ on $r=R$ and $\psi=0$ on $r=a$ can be built up exactly from the infinite-space Green function $\psi_\infty=(4\pi|\mathbf{r}-\mathbf{r}_o|)^{-1}$ using a standard cascade of images of the source point $\mathbf{r}_o$. Upon further averaging of the resulting Φ_1 throughout phase 1, we obtain to leading order in a/R (only the first two images of the infinite sequence are retained to this order),

$$L_1^2=\frac{9}{14}R^2\left[1-\frac{7}{6}\frac{a}{R}+O(a^3/R^3)\right]. \tag{50}$$

This estimate of L_1 will be used in the numerical results of the final section. Note that all reference to R may be eliminated using the phase 2 volume fraction $v_2=(a/R)^3$ or $R=av_2^{-1/3}$. In this case,

$$L_1^2=\tfrac{9}{14}a^2v_2^{-2/3}[1-\tfrac{7}{6}v_2^{1/3}+O(v_2)]. \tag{51}$$

B. High-frequency limit

If the applied confining pressure is changing at sufficiently high frequencies, the fluid pressure from the constituent with the higher average fluid pressure has time to invade only a small distance into the lower-pressure phase. In the limit $\omega\to\infty$, the fluid-pressure penetration can always be modeled as a locally one-dimensional process in the vicinity of $\partial\Omega_{12}$.

To study this limit, we employ a set of curvilinear coordinates (x,y,z) having metrical coefficients h_x,h_y,h_z in which the surface $x=0$ defines the interface $\partial\Omega_{12}$ and where $x>0$ corresponds locally to phase 1. We assume that as $|x|\to 0$ from either side, the metrical coefficients become independent of x; i.e., sufficiently close to $x=0$, the curvilinear coordinates become a set of "normal coordinates" in which x/h_x is a simple coordinate of linear distance even though y and z remain curvilinear. As $\omega\to\infty$, the solution of Eq. (9) takes the form (cf. Ref. [7])

$$p_{f1}(x,y,z)=p_{f1}^{\text{out}}(x,y,z)+C_1(y,z)e^{i\sqrt{i\omega/D_1}x/h_x}, \tag{52}$$

$$p_{f2}(x,y,z)=p_{f2}^{\text{out}}(x,y,z)+C_2(y,z)e^{-i\sqrt{i\omega/D_2}x/h_x}, \tag{53}$$

where the diffusivities D_i are defined as

$$D_i=\frac{k_i}{\eta}\frac{B_iK_i}{\alpha_i} \quad \text{for} \quad i=1,2, \tag{54}$$

and where the outer fluid-pressure fields that hold everywhere except in a vanishingly small neighborhood $\sqrt{D_i/\omega}$ of the interface $\partial\Omega_{12}$ are defined as the undrained response $p_{fi}^{\text{out}}=B_ip_{ci}^{\text{out}}$. The constants C_1 and C_2 will be determined presently from the continuity conditions on $x=0$.

Upon introducing $p_{fi}^{\text{out}}=B_ip_{ci}^{\text{out}}$ and the scaled displacements $\mathbf{u}_i^\infty(\mathbf{r})=-(1-\alpha_iB_i)\Delta P\mathbf{s}_i^\infty(\mathbf{r})/K_i$ into Eq. (14), the outer confining pressures may be written as

$$p_{ci}^{\text{out}} = \Delta P \nabla \cdot \mathbf{s}_i^{\infty}, \tag{55}$$

$$p_{fi}^{\text{out}} = B_i \Delta P \nabla \cdot \mathbf{s}_i^{\infty}. \tag{56}$$

The applied-force-independent displacements $\mathbf{s}_i^{\infty}$ satisfy

$$\mu_i^{\infty} \nabla^2 \mathbf{s}_i^{\infty} + \left(1 + \frac{\mu_i^{\infty}}{3}\right) \nabla \nabla \cdot \mathbf{s}_i^{\infty} = 0, \tag{57}$$

subject to the boundary condition on $\partial\Omega_i$

$$\mu_i^{\infty} \mathbf{n} \cdot (\nabla \mathbf{s}_i^{\infty} + \nabla \mathbf{s}_i^{\infty T} - \tfrac{2}{3} \nabla \cdot \mathbf{s}_i^{\infty} \mathbf{I}) + \nabla \cdot \mathbf{s}_i^{\infty} \mathbf{n} = \mathbf{n}, \tag{58}$$

and to the continuity conditions on $\partial\Omega_{12}$

$$[\mu_i^{\infty} \mathbf{n} \cdot (\nabla \mathbf{s}_i^{\infty} + \nabla \mathbf{s}_i^{\infty T} - \tfrac{2}{3} \nabla \cdot \mathbf{s}_i^{\infty} \mathbf{I}) + \nabla \cdot \mathbf{s}_i^{\infty} \mathbf{n}] = 0, \tag{59}$$

$$\left[\frac{\mu_i^{\infty}}{G_i} \mathbf{s}_i^{\infty}\right] = \mathbf{0}. \tag{60}$$

The parameter $\mu_i^{\infty} \equiv (1 - \alpha_i B_i) G_i / K_i$ is the dimensionless shear coefficient appropriate at high frequencies. As at low-frequencies, even though each porous constituent is uniform throughout the averaging volume, the local frame dilatations $\nabla \cdot \mathbf{s}_i^{\infty}$ need not be uniform in general.

To determine the coefficients $C_1(y,z)$ and $C_2(y,z)$, we employ the fluid-flow continuity conditions of Eq. (21) on $\partial\Omega_{12}$

$$\left[k_i h_x \frac{\partial p_{fi}^{\text{out}}}{\partial x} + i^{3/2} \sqrt{\omega} \frac{k_i}{\sqrt{D_i}} C_i\right] = 0, \tag{61}$$

$$[p_{fi}^{\text{out}} + C_i] = 0. \tag{62}$$

In the limit $\omega \to \infty$, the terms proportional to $\partial p_{fi}^{\text{out}} / \partial x$ are negligible so that

$$C_1 = -\frac{k_2 / \sqrt{D_2}}{k_1 / \sqrt{D_1} + k_2 / \sqrt{D_2}} [p_{f1}^{\text{out}} - p_{f2}^{\text{out}}], \tag{63}$$

$$C_2 = \frac{k_1 / \sqrt{D_1}}{k_1 / \sqrt{D_1} + k_2 / \sqrt{D_2}} [p_{f1}^{\text{out}} - p_{f2}^{\text{out}}], \tag{64}$$

where the outer pressure fields are being evaluated along $x = 0$. Using the definition of $\dot{\zeta}_{\text{int}}$ [Eq. (27) of Paper I] then gives that as $\omega \to \infty$,

$$-i\omega \zeta_{\text{int}} \sim \frac{i^{3/2} \sqrt{\omega}}{\eta} \frac{(k_1 / \sqrt{D_1})(k_2 / \sqrt{D_2})}{k_1 / \sqrt{D_1} + k_2 / \sqrt{D_2}} \times \frac{S}{V} [\langle p_{f1}^{\text{out}} \rangle_s - \langle p_{f2}^{\text{out}} \rangle_s], \tag{65}$$

where $\langle\ \rangle_s$ denotes an average over the interface region $\partial\Omega_{12}$, and where S is the total area of $\partial\Omega_{12}$ contained within the averaging region of volume V.

There is no reason, in general, why the surface average $\langle p_{fi}^{\text{out}} \rangle_s$ must be equal to the volume average $\overline{p_{fi}^{\text{out}}}$ for small volumes (but for large volumes it is expected that the two values will converge). Thus, we use $p_{fi}^{\text{out}} = B_i \Delta P \nabla \cdot \mathbf{s}_i^{\infty}$ to define the dimensionless material property

$$\theta = \frac{\langle p_{f1}^{\text{out}} \rangle_s - \langle p_{f2}^{\text{out}} \rangle_s}{\overline{p_{f1}^{\text{out}}} - \overline{p_{f2}^{\text{out}}}} \tag{66}$$

$$= \frac{S^{-1} \int_{\partial\Omega_{12}} (B_1 \nabla \cdot \mathbf{s}_1^{\infty} - B_2 \nabla \cdot \mathbf{s}_2^{\infty}) dS}{V_1^{-1} \int_{\Omega_1} B_1 \nabla \cdot \mathbf{s}_1^{\infty} dV - V_2^{-1} \int_{\Omega_2} B_2 \nabla \cdot \mathbf{s}_2^{\infty} dV}. \tag{67}$$

With this definition, we again obtain the transport law $-i\omega \zeta_{\text{int}} = \gamma(\omega)[\overline{p}_{f1} - \overline{p}_{f2}]$ of interest but now with an asymptotic frequency dependence given by

$$\gamma(\omega) \sim \frac{i^{3/2} \sqrt{\omega}}{\eta} \frac{(k_1 / \sqrt{D_1})(k_2 / \sqrt{D_2})}{k_1 / \sqrt{D_1} + k_2 / \sqrt{D_2}} \frac{S}{V} \theta \tag{68}$$

as $\omega \to \infty$. Thus, the fluid volume ζ_{int} exchanged between the two phases tends to zero as $1/\sqrt{\omega}$ in the limit as $\omega \to \infty$.

For those special cases considered earlier in which the strains $\nabla \cdot \mathbf{s}_i^{\infty}$ are uniform throughout the composite (e.g., when $G_1 = G_2$ or for certain conformally layered composites including rectangular networks of thin joints) we find that $\theta = 1$, and that θ also approaches unity in general when the volume becomes very large.

C. Full model for $\gamma(\omega)$

To connect the low- and high-frequency behavior of $\gamma(\omega)$, we use the simple function

$$\gamma(\omega) = \gamma_o \sqrt{1 - i\frac{\omega}{\omega_c}}, \tag{69}$$

where the relaxation frequency ω_c is defined as

$$\omega_c = \left[\eta \left(\frac{\sqrt{D_1}}{k_1} + \frac{\sqrt{D_2}}{k_2}\right) \frac{V}{S} \frac{\gamma_o}{\theta}\right]^2 \tag{70}$$

$$= \frac{\eta B_1 K_1}{k_1 \alpha_1} \left(\frac{V}{S} \frac{\gamma_o}{\theta}\right)^2 \left(1 + \sqrt{\frac{k_1 B_2 K_2 \alpha_1}{k_2 B_1 K_1 \alpha_2}}\right)^2. \tag{71}$$

Equations (69) and (71), along with Eq. (49) for γ_o, are the results of interest here. As required for a causal response, any zeros or singularities of either $\gamma(\omega)$ or $1/\gamma(\omega)$ must lie in the lower half of the complex-ω plane when there is an assumed $e^{-i\omega t}$ time dependence; i.e., both $\gamma(\omega)$ and $1/\gamma(\omega)$ must be analytic everywhere in the upper-half ω plane including the entire real ω axis. The above model for $\gamma(\omega)$ satisfies these important constraints since the only singularity is a branch point at $\omega = -i\omega_c$. Finally, since the inverse transform of $\gamma(\omega)$ must be the real function $\Gamma(t)$, we must have $\gamma(\omega)^* = \gamma(-\omega^*)$, which is also seen to be satisfied by formula (69).

In practice, the square-root term in Eq. (71) can be neglected relative to unity in any situation where a double-porosity theory is likely to be necessary (both k_1/k_2 and

K_2/K_1 are small). We will normally assume that $\theta \approx 1$ as well, with γ_o given by Eq. (49).

III. MACROSCOPIC FLOW LAWS

A. Problem statement

We imagine an averaging volume in the form of a circular disk with sealed boundary conditions on the outer circumferential face and fluid-pressure boundary conditions applied to the two flat faces. The axis of this disk is defined as the z direction so that the two flat faces reside at $z=-H$ and $z=H$.

We consider two applied forcing states, the sum of which gives the total flux. In the first state, denoted with a superscript a, a pressure drop is applied across phase 1, while maintaining no pressure drop across phase 2:

$$p_{f1}^{a}(\mathbf{r})=\begin{cases}\Delta P_1, & z=H\\ -\Delta P_1, & z=-H,\end{cases} \quad p_{f2}^{a}(\mathbf{r})=\begin{cases}0, & z=H\\ 0, & z=-H.\end{cases} \tag{72}$$

In the second state, denoted with a superscript b, the pressure drop is applied to phase 2:

$$p_{f1}^{b}(\mathbf{r})=\begin{cases}0, & z=H\\ 0, & z=-H,\end{cases} \quad p_{f2}^{b}(\mathbf{r})=\begin{cases}\Delta P_2, & z=H\\ -\Delta P_2, & z=-H.\end{cases} \tag{73}$$

In writing these conditions, we have taken $\overline{p}_{f1,2}^{a,b}=0$. As is fairly straightforward to demonstrate (e.g., Ref. [9]), the boundary conditions of Eqs. (72) and (73) are equivalent to the presence of uniform force densities in each phase of the form $(\Delta P_{1,2}/H)\hat{\mathbf{z}}$. The frame of reference for the relative flow is the framework of grains that, in the presence of waves, is accelerating as $\dot{\mathbf{v}}$. Thus, in identifying the pressure drops ΔP_i, the uniform inertial force $\rho_f(\dot{\mathbf{v}}-\mathbf{g})$ must be included to give

$$\frac{\Delta P_i}{H}=\hat{\mathbf{z}}\cdot[\nabla\overline{p}_{fi}+\rho_f(\dot{\mathbf{v}}-\mathbf{g})]. \tag{74}$$

As per the treatment of Pride and Flekkoy [9], the identification in Eq. (74) is independent of both the average fluid pressure in each phase $\overline{p}_{fi}$ and the presence of volume-fraction gradients ∇v_i. The only requirement is that the volume fractions v_i be well approximated by the area fractions determined on the two flat faces

$$v_i=\frac{A_i(z=+H)+A_i(z=-H)}{2A}, \tag{75}$$

where A is the area of one of the two flat faces and where $A_i(z=\pm H)$ is the area of each flat face that is occupied by phase i. See Pride and Flekkoy [9] for a discussion of the conditions required for Eq. (75) to be a good approximation.

Further comment is in order when the applied pressure drops are changing in time as $e^{-i\omega t}$. For the problem of linear wave propagation through the composite, the fluid pressure gradients are created by compression of the framework of grains on time scales dictated by the compressional-wave speed. So long as the wavelengths of the compressional wave remain large relative to H, the identification of Eq. (74) remains valid (i.e., the macroscopic fluid pressure gradients are created essentially instantaneously relative to the time $1/\omega$). Other than for the overall pressure drop ΔP_i across each phase associated with the wavelength-scale variations of the fluid pressure, our modeling of $\dot{\zeta}_{\mathrm{int}}$ has already accounted for all aspects of the heterogeneous fluid pressure response in the composite. Thus, the local Darcy flow induced by the wave may properly be taken to be solenoidal ($\nabla\cdot\mathbf{Q}_i=0$) in the present section.

However, if laboratory measurements are performed by applying time harmonic pressures to fluid reservoirs that connect to the faces $z=\pm H$, then to use the present description for interpreting the measurements, the time $(2H)^2/D_i$ required to establish the macroscopic pressure gradient [where D_i is the fluid-pressure diffusivity defined in Eq. (54)] must be much smaller than $2\pi/\omega$. If $2H$ is taken to be the smallest length that contains within it the pertinent mesoscopic variation of the two constituents, then the maximum applied frequency f that can be treated is $f_{\max}=D_i/(8\pi H^2)$.

The governing equations that complement the above boundary conditions on the external surface are thus

$$\nabla^2 p_{fi}^{a,b}=0 \text{ in } \Omega_i, \tag{76}$$

$$p_{f1}^{a,b}=p_{f2}^{a,b} \text{ on } \partial\Omega_{12}, \tag{77}$$

$$\mathbf{n}\cdot\nabla p_{f2}^{a,b}=\epsilon\mathbf{n}\cdot\nabla p_{f1}^{a,b} \text{ on } \partial\Omega_{12}, \tag{78}$$

where $\epsilon(\omega)\equiv k_1(\omega)/k_2(\omega)$ is the ratio of the intrinsic permeabilities. The frequency dependence in the intrinsic permeabilities is again that due to the development of viscous boundary layers in the pores (a proper model having been given previously by Johnson *et al.* [6]). The elliptic problem presented by Eqs. (76)–(78) exhibits no frequency relaxation other than whatever is contained within $\epsilon(\omega)$.

Our averaging disk has a total volume of $V=2AH$. The definition of the macroscopic flux $\mathbf{q}_i^{a,b}$ [Eq. (22) of Paper I] that corresponds to the above problem is then

$$\mathbf{q}_2^{a,b}=-\frac{k_2}{\eta}\frac{\hat{\mathbf{z}}}{2A}\left[\int_{z=+H}\hat{\mathbf{z}}\cdot\nabla p_{f2}^{a,b}dS+\int_{z=-H}\hat{\mathbf{z}}\cdot\nabla p_{f2}^{a,b}dS\right], \tag{79}$$

$$\mathbf{q}_1^{a,b}=-\frac{k_2\epsilon}{\eta}\frac{\hat{\mathbf{z}}}{2A}\left[\int_{z=+H}\hat{\mathbf{z}}\cdot\nabla p_{f1}^{a,b}dS+\int_{z=-H}\hat{\mathbf{z}}\cdot\nabla p_{f1}^{a,b}dS\right]. \tag{80}$$

From the linearity of the physics as well as the assumed isotropy of the double-porosity composite, we can immediately write the macroscopic Darcy law as

$$\begin{bmatrix}\mathbf{q}_1\\ \mathbf{q}_2\end{bmatrix}=\begin{bmatrix}\mathbf{q}_1^{a}+\mathbf{q}_1^{b}\\ \mathbf{q}_2^{a}+\mathbf{q}_2^{b}\end{bmatrix} \tag{81}$$

$$= \frac{-1}{\eta}\begin{bmatrix} \kappa_{11} & \kappa_{12} \\ \kappa_{21} & \kappa_{22} \end{bmatrix}\begin{bmatrix} \nabla \overline{p}_{f1} + \rho_f(\dot{\mathbf{v}} - \mathbf{g}) \\ \nabla \overline{p}_{f2} + \rho_f(\dot{\mathbf{v}} - \mathbf{g}) \end{bmatrix}. \tag{82}$$

In terms of our above statement of the boundary-value problem, the four permeability coefficients are defined by

$$\frac{\kappa_{11}}{\eta} = \frac{|\hat{\mathbf{z}} \cdot \mathbf{q}_1^a|}{\Delta P_1 / H}, \quad \frac{\kappa_{12}}{\eta} = \frac{|\hat{\mathbf{z}} \cdot \mathbf{q}_1^b|}{\Delta P_2 / H},$$

$$\frac{\kappa_{21}}{\eta} = \frac{|\hat{\mathbf{z}} \cdot \mathbf{q}_2^a|}{\Delta P_1 / H}, \quad \frac{\kappa_{22}}{\eta} = \frac{|\hat{\mathbf{z}} \cdot \mathbf{q}_2^b|}{\Delta P_2 / H}. \tag{83}$$

B. Reciprocity

Using all of these results, the reciprocity condition $\kappa_{12} = \kappa_{21}$ will now be proven. We first form the products

$$p_{f1}^b[\nabla^2 p_{f1}^a] \quad \text{and} \quad p_{f1}^a[\nabla^2 p_{f1}^b], \tag{84}$$

both of which vanish from Eq. (76). Equivalent expressions (replace 1 with 2) hold for phase 2. Taking the difference of these expressions gives

$$\nabla \cdot [p_{f1}^b \nabla p_{f1}^a - p_{f1}^a \nabla p_{f1}^b] = 0, \tag{85}$$

which upon integrating over Ω_1, dividing by $V = 2AH$, and appealing to the divergence theorem and the boundary conditions of Eqs. (72) and (73) yields

$$\frac{\Delta P_1}{H}\frac{1}{2A}\left[\int_{z=+H} \hat{\mathbf{z}} \cdot \nabla p_{f1}^b dS + \int_{z=-H} \hat{\mathbf{z}} \cdot \nabla p_{f1}^b dS\right]$$

$$= -\frac{1}{V}\int_{\Omega_{12}} \mathbf{n} \cdot [p_{f1}^b \nabla p_{f1}^a - p_{f1}^a \nabla p_{f1}^b] dS. \tag{86}$$

Using Eq. (80) for the definition of the macroscopic flux along with the above definition of κ_{12} allows us to write

$$\frac{\Delta P_1 \Delta P_2}{H^2}\frac{\eta}{k_2}\kappa_{12} = -\frac{\epsilon}{V}\int_{\Omega_{12}} \mathbf{n} \cdot [p_{f1}^b \nabla p_{f1}^a - p_{f1}^a \nabla p_{f1}^b] dS. \tag{87}$$

Identical manipulations for phase 2 gives

$$\frac{\Delta P_1 \Delta P_2}{H^2}\frac{\eta}{k_2}\kappa_{21} = \frac{1}{V}\int_{\Omega_{12}} \mathbf{n} \cdot [p_{f2}^a \nabla p_{f2}^b - p_{f2}^b \nabla p_{f2}^a] dS. \tag{88}$$

If these two equations are subtracted and the continuity conditions of Eqs. (77) and (78) employed, one indeed finds that $\kappa_{12} = \kappa_{21}$. Such a simple proof of the reciprocity is not forthcoming if the volume-averaged flow fields $v_i \overline{\mathbf{Q}}_i$ are used in place of the mean fluxes $\mathbf{q}_i$.

C. Permeability matrix

In order to obtain a model for the κ_{ij} that has separable contributions from the mesoscopic geometry of the constituents and from the underlying material properties [which are here entirely contained in $\epsilon(\omega)$, as defined after Eq. (78)], it is assumed that in practice, ϵ is a small number. The need to use a double-porosity theory is apparent precisely when ϵ is a small number.

We are now able to develop the fluid pressures as

$$p_{fi}^a = [\varphi_i^a + \epsilon \pi_i^a + O(\epsilon^2)]\Delta P_1 / H, \tag{89}$$

$$p_{fi}^b = [\varphi_i^b + \epsilon \pi_i^b + O(\epsilon^2)]\Delta P_2 / H, \tag{90}$$

where the applied-force-independent potentials $\varphi_i^{a,b}$ and $\pi_i^{a,b}$ have units of length, and are dependent only on the mesoscopic geometry of the two porous constituents. Because the local Darcy flow in phase 1 goes as $\mathbf{Q}_1 = -\epsilon k_2 \nabla p_{f1} / \eta$, the leading-order flow in ϵ is independent of the potentials $\pi_1^{a,b}$. The leading-order potentials are all solutions of Laplace's equation in their respective phases and from Eqs. (76)–(78) satisfy the following boundary conditions:

$$\mathbf{n} \cdot \nabla \varphi_2^a = 0 \quad \text{on} \quad \partial\Omega_{12}, \quad \varphi_2^a = \begin{cases} 0, & z = H \\ 0, & z = -H; \end{cases}$$

$$\varphi_1^a = 0 \quad \text{on} \quad \partial\Omega_{12}, \quad \varphi_1^a = \begin{cases} H, & z = H \\ -H, & z = -H; \end{cases}$$

$$\mathbf{n} \cdot \nabla \varphi_2^b = 0 \quad \text{on} \quad \partial\Omega_{12}, \quad \varphi_2^b = \begin{cases} H, & z = H \\ -H, & z = -H; \end{cases}$$

$$\mathbf{n} \cdot \nabla \pi_2^{a,b} = \mathbf{n} \cdot \nabla \varphi_1^{a,b} \quad \text{on} \quad \partial\Omega_{12}, \quad \pi_2^{a,b} = \begin{cases} 0, & z = H \\ 0, & z = -H; \end{cases}$$

$$\varphi_1^b = \varphi_2^b \quad \text{on} \quad \partial\Omega_{12}, \quad \varphi_1^b = \begin{cases} 0, & z = H \\ 0, & z = -H. \end{cases} \tag{91}$$

Since φ_2^a satisfies homogeneous boundary conditions, it has the unique solution that $\varphi_2^a = 0$ everywhere, and this is why $\varphi_1^a = \varphi_2^a = 0$ on $\partial\Omega_{12}$.

Thus, using these potentials in the definitions of Eqs. (79), (80), and (83), it is a straightforward excercise (integrate, use the divergence theorem, appeal to the boundary conditions) to write the κ_{ij} in the following forms to leading order:

$$\kappa_{11}/k_2 = \epsilon \langle \nabla \varphi_1^a \cdot \nabla \varphi_1^a \rangle, \tag{92}$$

$$\kappa_{12}/k_2 = \epsilon \langle \nabla \varphi_1^a \cdot \nabla \varphi_1^b \rangle, \tag{93}$$

$$\kappa_{22}/k_2 = \langle \nabla \varphi_2^b \cdot \nabla \varphi_2^b \rangle + \epsilon \langle \nabla \Phi_2^b \cdot \nabla \pi_2^b \rangle, \tag{94}$$

where the brackets indicate a volume average over the entire averaging volume. These averages are dimensionless order-unity functions of the mesoscopic geometry of the constituents. In the second term of κ_{22}, the potential Φ_2^b is a solution to Laplace's equation in phase 2 satisfying $\Phi_2^b = 0$ on $\partial\Omega_{12}$ and $\Phi_2^b = \pm H$ on $z = \pm H$.

Even for the simple "plane-parallel-joint" geometry depicted in Fig. 1 for the case of forcing-state *a*, the dimensionless field $\nabla \varphi_1^a$ is not just the unit vector $\hat{\mathbf{z}}$. Indeed, rather

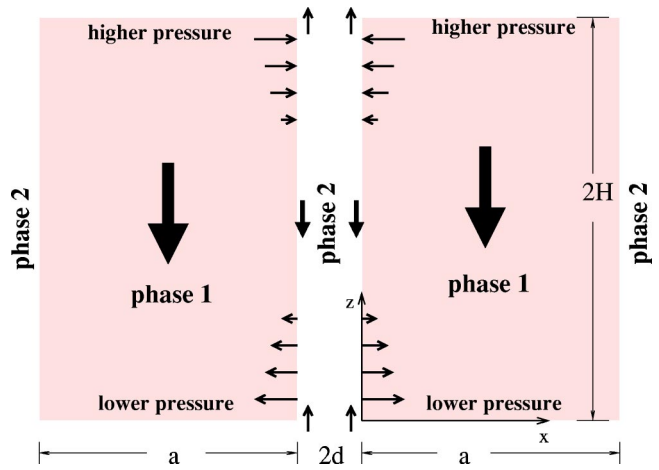

FIG. 1. An idealized unsealed double-porosity sample has the same average fluid pressure in both phases, but there is a macroscopic pressure gradient in the vertical direction $\hat{\mathbf{z}}$ across phase 1 driving a flow in phase 1 (the large arrows) while we impose the boundary condition that no pressure gradient can develop across phase 2. Nonetheless, there is induced in phase 2 secondary local flow including flow across the internal surface $\partial\Omega_{12}$ as indicated by the small arrows. The analytically determined fluid pressure distribution for this situation is shown in Fig. 2.

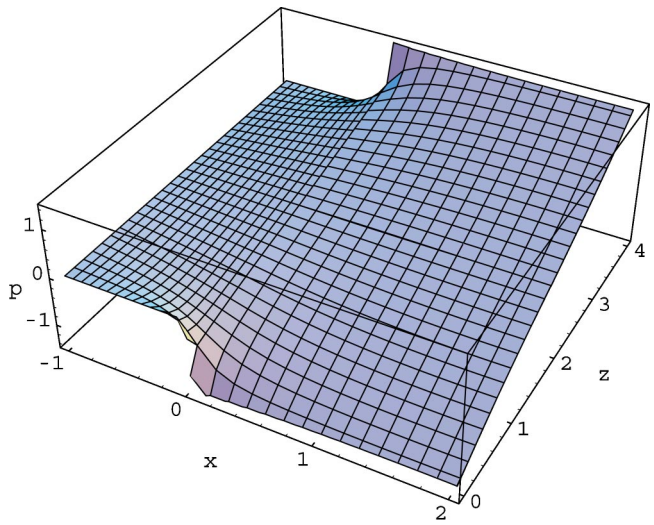

FIG. 2. A plot of the normalized fluid pressure p for the geometry depicted in Fig. 1 in which $d=1$, $a=4$, and $H=2$. The interface $\partial\Omega_{12}$ between the two phases is located at $x=0$ (and at $x=4$), while the plane $x=-1$ is at the midpoint of the joint phase and the plane $x=2$ is at the midpoint of the matrix phase. The permeability ratio ϵ has been taken to be 0.1. The pressure gradient has a singularity in the x direction at the points $(x=0,z=0)$ and $(x=0,z=2H=4)$.

nontrivial flow develops as indicated qualitatively by the arrows. Because there is a macroscopic pressure gradient across phase 1 and none across phase 2, there are fluid-pressure variations in the x direction that drive flow laterally either into or out of phase 2 as shown. The only trivial potential in this geometry is φ_2^b, which does correspond to $\nabla\varphi_2^b=\hat{\mathbf{z}}$.

To understand this flow better, we solve in the Appendix the asymptotic (leading order in ϵ) flow problem corresponding to forcing state a, i.e., we determine the pressure fields $p_{f1}^a=\varphi_1^a$ and $p_{f2}^a=\epsilon\pi_2^a$ that contribute to the leading-order Darcy flow. The results are plotted in Fig. 2. We see indeed that there is considerable cross flow between the phases (which averages to zero throughout the entire sample so that $\dot{\zeta}_{\text{int}}=0$ always). At the entrance of the sample (taken as $z=4$ in the figure), we see that fluid is flowing out of phase 2 while at the exit $(z=0)$, fluid is flowing into phase 2; i.e., such flow is in the opposite direction to the average phase-1 flow.

The permeability matrix is finally written in a slightly different form. The phase-1 potential φ_1^a, that satisfies Dirichlet conditions on $\partial\Omega_{12}$, is rewritten as $\varphi_1^a=\psi_1^a+\delta\varphi_1^a$, where ψ_1^a satisfies the Neumann condition $\mathbf{n}\cdot\nabla\psi_1^a=0$ on $\partial\Omega_{12}$ and $\psi_1^a=\pm H$ on $z=\pm H$ and where the difference potential $\delta\varphi_1^a$ therefore satisfies $\delta\varphi_1^a=-\psi_1^a$ on $\partial\Omega_{12}$ and $\delta\varphi_1^a=0$ on $z=\pm H$. Similarly, the phase-2 potential Φ_2^b satisfying Dirichlet conditions on $\partial\Omega_{12}$ is rewritten as $\Phi_2^b=\varphi_2^b+\delta\varphi_2^b$ so that the difference potential satisfies $\delta\varphi_2^b=-\varphi_2^b$ on $\partial\Omega_{12}$ and $\delta\varphi_2^b=0$ on $z=\pm H$. Using these potentials in Eqs. (92)–(94), the permeability matrix takes the form

$$\kappa_{ij}=k_2\begin{bmatrix}\epsilon(1/F_1+\chi_{11}) & -\epsilon\chi_{12}\\ -\epsilon\chi_{12} & 1/F_2+\epsilon\chi_{22}\end{bmatrix}, \tag{95}$$

where F_i are the formation factors of each phase defined using the Neumann potentials as

$$1/F_1=\langle\nabla\psi_1^a\cdot\nabla\psi_1^a\rangle$$

and

$$1/F_2=\langle\nabla\varphi_2^b\cdot\nabla\varphi_2^b\rangle \tag{96}$$

and where the parameters χ_{ij} are defined as

$$\chi_{11}=\langle\nabla\delta\varphi_1^a\cdot\nabla\delta\varphi_1^a\rangle, \tag{97}$$

$$-\chi_{12}=\langle\nabla\delta\varphi_1^a\cdot\nabla\varphi_1^b\rangle, \tag{98}$$

$$\chi_{22}=\langle\nabla\delta\varphi_2^b\cdot\nabla\pi_2^b\rangle. \tag{99}$$

One of the principal reasons for writing the permeability matrix in this form is that in any plane-parallel joint model, the two Neumann potentials are equal along the internal interface, i.e., $\psi_1^a=\varphi_2^b$ on $\partial\Omega_{12}$. Using this fact, it is straightforward to use the boundary conditions on $\partial\Omega_{12}$ along with Eqs. (97)–(99) to show that $\chi_{11}=\chi_{12}=\chi_{22}\equiv\chi$ for such models.

Flow in plane-parallel joint models thus has the interesting property that the total flow $\mathbf{q}_1+\mathbf{q}_2$ is unaffected by the cross-coupling coefficient χ. However, the energy-dissipation rate σ due to the Darcy flow,

$$\sigma=\frac{\epsilon(1/F_1+\chi)}{\eta}\nabla\overline{p}_{f1}\cdot\nabla\overline{p}_{f1}-\frac{2\epsilon\chi}{\eta}\nabla\overline{p}_{f1}\cdot\nabla\overline{p}_{f2}+\frac{(1/F_2+\epsilon\chi)}{\eta}\nabla\overline{p}_{f2}\cdot\nabla\overline{p}_{f2},\tag{100}$$

is seen to be affected by χ when $\nabla\overline{p}_{f1}\neq\nabla\overline{p}_{f2}$. In other-words, the extra influx and outflux of fluid, as seen in Figs. 1 and 2, at the entrance and exit faces is *dissipating energy* even if it is not contributing to the total flow.

Using the results from the Appendix for flow in the two-dimensional (2D) geometry of Fig. 1, and taking a square of material in which $2H=a+2d$, we find Eq. (95) with $1/F_i=v_i$ and with $\chi_{11}=\chi_{12}=\chi_{22}=(2/\pi)\Sigma_{n=1}^{\infty}\tanh(n\pi v_1)/n$. Unfortunately, this series is logarithmically divergent, which can be seen in the limit $n\to\infty$, where it becomes the harmonic series $\Sigma_n 1/n$, which is well known to diverge. This divergence is entirely due to those points where the internal surface $\partial\Omega_{12}$ and the two flat faces $z=\pm H$ meet (e.g., the points $x=0$, $z=0$ and $x=0$, $z=4$ in Fig. 2). At such points, there is a discontinuous jump in the fluid-pressure boundary conditions, resulting in locally divergent flow. This nonphysical artifact can be removed by requiring the potentials on the boundaries to vary smoothly at those points where the internal surface intersects the flat faces. The smoothing distance can be made arbitarily small relative to the joint thickness d but, so long as it remains finite, the permeability matrix retains the form of Eq. (95) and has a finite χ. Elaboration of this rather involved demonstration is left to the interested reader.

IV. CONCLUSIONS

The main result of the present paper is the frequency and material-property dependencies of the internal transport coefficient $\gamma(\omega)$, as expressed in Eqs. (69)–(71). The coefficient $\gamma(\omega)$ controls the mesoscopic fluid-pressure equilibration between the two porous constituent phases. We have also established that the dual-permeability Darcy law is symmetric. The cross coupling in the Darcy law was shown to be due to the existence of local fluid-pressure gradients that drive flow from one porous phase to the other.

ACKNOWLEDGMENTS

The work of J.G.B. was performed under the auspices of the U.S. Department of Energy under Contract No. W-7405-ENG-48 and supported specifically by the Geosciences Research Program of the DOE Office of Basic Energy Sciences, Division of Chemical Sciences, Geosciences and Biosciences.

APPENDIX: 2D FLOW THROUGH A PLANAR SLAB GEOMETRY

We now obtain the fluid pressure distribution for the simple 2D flow geometry presented in Fig. 1. The pressures are obtained to leading order in $\epsilon=k_1/k_2$ as

$$p_{f1}^a=(\varphi_1^a+\epsilon\pi_1^a)\Delta P_1/H,$$

$$p_{f2}^a=\epsilon\pi_2^a\Delta P_1/H,$$

$$p_{f1}^b=(\varphi_1^b+\epsilon\pi_1^b)\Delta P_2/H,$$

$$p_{f2}^b=(z+\epsilon\pi_2^b)\Delta P_2/H.$$

Since the pressure gradient in phase 1 gets multiplied by another factor of ϵ when determining the flow, we need only determine the four potentials φ_1^a, π_2^a, φ_1^b, and π_2^b if our interest is to understand the pressure field giving rise to the leading-order flow. These potentials are all solutions of Laplace's equation and satisfy the boundary conditions given in Eq. (91). Phase 1 is taken to lie between $0\leqslant x\leqslant a$ and phase 2 between $-2d\leqslant x\leqslant 0$.

The solution of the Laplace equation in 2D is the sum of products of the form $[\sin ax,\cos bx]\times[\sinh cz,\cosh dz]$. For example, φ_1^a has a solution of the form

$$\varphi_1^a(x,z)=\sum_{n=1}^{\infty}A_n\sin\left(\frac{\pi nx}{a}\right)\times\frac{\{\sinh[\pi n(z+H)/a]+\sinh[\pi n(z-H)/a]\}}{\sinh[\pi n2H/a]},$$

satisfying the required Dirichlet conditions at $x=0$ and $x=a$. The constants A_n are selected so that the nonhomogeneous conditions at $z=\pm H$ are satisfied and this is done in the usual manner by exploiting the completeness relation for the sine basis functions. We find (cf. Morse and Feshbach [10], p. 708).

$$\varphi_1^a=\frac{4H}{\pi}\sum_{n\ \mathrm{odd}}^{\infty}\frac{1}{n}\sin\left(\frac{\pi nx}{a}\right)\times\frac{\{\sinh[\pi n(z+H)/a]+\sinh[\pi n(z-H)/a]\}}{\sinh[\pi n2H/a]}.\tag{A1}$$

The other potentials are similarly found to be

$$\pi_2^a=\frac{-2H}{\pi}\sum_{n=1}^{\infty}\frac{(-1)^n}{n}\sin\left(\frac{\pi nz}{H}\right)\tanh\left(\frac{\pi na}{2H}\right)\times\frac{\{\cosh[\pi n(x+2d)/H]+\cosh[\pi nx/H]\}}{\sinh[\pi n2d/H]},\tag{A2}$$

$$\varphi_1^b=\frac{-2H}{\pi}\sum_{n=1}^{\infty}\frac{(-1)^n}{n}\sin\left(\frac{\pi nz}{H}\right)\times\frac{\{\sinh[\pi n(a-x)/H]+\sinh[\pi nx/H]\}}{\sinh[\pi na/H]},\tag{A3}$$

and

$$\pi_2^b = \frac{-2H}{\pi} \sum_{n=1}^{\infty} \frac{(-1)^n}{n} \sin\left(\frac{\pi n z}{H}\right) \frac{1-\cosh(\pi n a/H)}{\sinh[\pi n a/H]} \times \frac{\{\cosh[\pi n(x+2d)/H] + \cosh[\pi n x/H]\}}{\sinh[\pi n 2d/H]}. \quad \text{(A4)}$$

These potentials are those contributing to the pressure distribution in Fig. 2.

The quantities needed for estimating the permeabilities are the integrals of the z derivatives of these potentials on the external surface. One finds that

$$\int_0^a dx \frac{\partial \varphi_1^a}{\partial z} = a + \chi, \quad \text{(A5)}$$

$$\int_{-2d}^0 dx \frac{\partial \pi_2^a}{\partial z} = -\int_{-2d}^0 dx \frac{\partial \pi_2^b}{\partial z} = \int_0^a dx \frac{\partial \varphi_1^b}{\partial z} = -\chi, \quad \text{(A6)}$$

where the parameter χ is defined as

$$\chi = \frac{4H}{\pi} \sum_{n=1}^{\infty} \frac{1}{n} \tanh\left(\frac{\pi n a}{2H}\right). \quad \text{(A7)}$$

This series is logarithmically divergent for reasons discussed in the text, but finite results are obtained by introducing a physically motivated smoothing distance.

[1] M.A. Biot, J. Acoust. Soc. Am. **28**, 168 (1956).
[2] M.A. Biot, J. Appl. Phys. **33**, 1482 (1962).
[3] J.G. Berryman and H.F. Wang, Int. J. Rock Mech. Min. Sci. **37**, 63 (2000).
[4] S.R. Pride and J.G. Berryman, Phys. Rev. E **68**, 036603 (2003), preceding paper.
[5] S.R. deGroot and P. Mazur, *Non-equilibrium Thermodynamics* (Dover, New York, 1984).
[6] D.L. Johnson, J. Koplik, and R. Dashen, J. Fluid Mech. **176**, 379 (1987).
[7] D.L. Johnson, J. Acoust. Soc. Am. **110**, 682 (2001).
[8] A.W. Skempton, Geotechnique **4**, 143 (1954).
[9] S.R. Pride and E.G. Flekkoy, Phys. Rev. E **60**, 4285 (1999).
[10] P.M. Morse and H. Feshbach, *Methods of Theoretical Physics, Parts I and II* (McGraw-Hill, New York, 1953).